

哑铃形高功率全保偏大模场掺镱锁模光纤激光器

陈河^{1*}, 周峰¹, 雷成敏¹, 蔡君豪², 陈胜平²¹中国人民解放军 93236 部队, 北京 100085;²国防科技大学前沿交叉学科学院, 湖南 长沙 410073

摘要 采用基于非线性光纤环形镜的哑铃形结构搭建了全光纤全保偏掺镱锁模激光器。通过使用全保偏大模场光纤、高功率光纤器件和优化的腔结构, 实现了脉冲宽度在 156 ps 到 8.1 ns 范围内可调的高功率、大能量矩形耗散孤子共振脉冲输出, 在最大泵浦功率 22.7 W 下激光器直接输出功率达到 5.5 W, 脉冲能量达到 0.68 μJ , 峰值功率为 84 W。得益于全保偏光纤结构, 所设计的激光器具有出色的抗干扰性和稳定性。

关键词 激光器; 光纤激光器; 锁模激光器; 耗散孤子共振; 非线性光学环形镜; 哑铃形激光器

中图分类号 TN248

文献标志码 A

doi: 10.3788/CJL202148.0315003

被动锁模光纤激光器由于具有结构简单、成本低、可靠性高等优势被广泛研究。特别是全光纤被动锁模光纤激光器, 由于没有空间光学元件, 在稳定性、可靠性以及封装工艺上有突出优势, 但受限于光纤非线性和器件功率承受能力等, 脉冲能量和平均功率普遍较低。近些年被广泛研究的耗散孤子共振 (dissipative soliton resonance, DSR) 锁模具有脉冲能量随增益线性增加的特性, 被认为是提高光纤锁模激光器脉冲能量和功率的关键途径^[1]。目前高功率大能量 DSR 锁模激光器大部分都采用基于非线性光学环形镜 (nonlinear optical loop mirror, NOLM) 或非线性偏振旋转的非保偏结构。其中, Huang 等^[2] 和 Guo 等^[3] 分别报道了最大功率为 2 W、脉冲能量为 232 nJ 和最大功率为 2.4 W、脉冲能量为 237 nJ 的全光纤 DSR 掺镱锁模激光器。非保偏结构一般都需要反复调试偏振控制器才能实现稳定锁模, 且锁模状态受环境变化影响; 而全保偏结构则具有免调试锁模启动、抗干扰能力强和稳定性高的优势^[4-6]。目前全光纤全保偏 DSR 锁模激光器报道较少^[7]。前期, 本课题组为了解决传统 8 字形激光器中的隔离器易受损、自启动难等问题, 在类似结构的基础上提出了基于双 NOLM 的哑铃形锁

模激光器结构^[8-9], 该结构在产生大能量、高功率锁模脉冲方面有独特优势, 同时容易实现全保偏化^[10]。为进一步提升全光纤锁模激光器直接输出脉冲的能量和功率, 同时保证激光器具有较强的抗干扰性和较高的稳定性, 本文基于全保偏哑铃形结构, 通过使用全保偏大模场光纤、高功率光纤器件, 并优化腔结构参数, 实现了全光纤谐振腔直接产生最高功率大于 5 W、波长为 1.06 μm 、脉冲宽度在 ps 至 ns 量级可调的耗散孤子共振脉冲, 在最高泵浦功率下, 输出脉冲宽度为 8.1 ns, 脉冲能量达到 0.68 μJ 。该激光器作为级联放大器的种子源可减少 1~2 级预先放大级, 明显简化结构, 缩减成本。同时, 采用全保偏结构可实现免调试锁模启动和高稳定性运转。

激光器结构如图 1(a) 所示, 主要包括放大器和两端 NOLM 组成的等效腔镜。左侧的 NOLM1 耦合比为 10 : 90, 环中接入一个具有 $3\pi/4$ 相移的非互易相移器 (non-reciprocal phase shifter, NRPS), 并将腔外自由端口作为激光器的输出端口; 右侧的 NOLM2 耦合比为 50 : 50, 环中接入中心波长为 1064 nm、3 dB 带宽为 13 nm 的带通滤波器。在激光器中间线性腔段内加入一段 2 m 长的双包层保偏掺

收稿日期: 2020-12-02; 修回日期: 2020-12-21; 录用日期: 2020-12-28

基金项目: 国家自然科学基金(61705267)

* E-mail: chenhe@qq.com

镜光纤作为增益介质,纤芯包层直径分别为 $10\ \mu\text{m}$ 和 $125\ \mu\text{m}$, $976\ \text{nm}$ 处的吸收系数为 $4.8\ \text{dB/m}$ 。泵浦光由最大功率为 $22.7\ \text{W}$ 的 $976\ \text{nm}$ 多模半导体激光器提供,通过 $(2+1)\times 1$ 的保偏合束器耦合到增益光纤的包层。腔内所有其他无源光纤都采用纤芯直径为 $10\ \mu\text{m}$ 、数值孔径为 0.08 的双包层大模场单模保偏光纤,相比于一般方案采用的小模场单包层光纤,其模场面积增大了 2 倍,非线性系数减小了 $2/3$,可以减弱腔内非线性效应的强度,在同等条件下可容纳更高的峰值功率和脉冲能量。NOLM1 的环长约 $5\ \text{m}$,NOLM2 的环长约 $4.5\ \text{m}$,线性腔的腔长约为 $7.5\ \text{m}$,当工作波长为 $1064\ \text{nm}$ 时腔内为全正色散,总色散约为 $0.5\ \text{ps}^2$,对应的锁模脉冲重复频率约为 $8\ \text{MHz}$ 。NOLM1 同时起到等效输出腔镜和等效饱和吸收体的作用,而 NOLM2 中加入的

带通滤波器在稳定激光中心波长和形成耗散孤子共振的过程中发挥关键作用。NOLM1 的 NRPS 采用图 1(b)所示的全光纤封装结构,通过法拉第转子的非互易旋光特性,使正向通过和反向通过 NRPS 的相移量不同,并通过中间的波片控制相移差。NRPS 的加入可以改变反射式 NOLM 的功率相关反射率曲线,使其具有饱和吸收特性,而且合理选择 NRPS 的相移大小,还可以改变基于 NOLM 的锁模激光器锁模的自启动性能。本实验选择了具有 $3\pi/4$ 相移的 NOLM,相比于 $\pi/2$ 相移的 NOLM,具有更大的调制深度值;相比于 π 相移的 NOLM,具有更低的锁模启动阈值。由于激光器中 NOLM2 使用耦合比为 $50:50$ 的耦合器,相当于全反镜,该结构也被认为是 9 字形激光器的特殊形式。

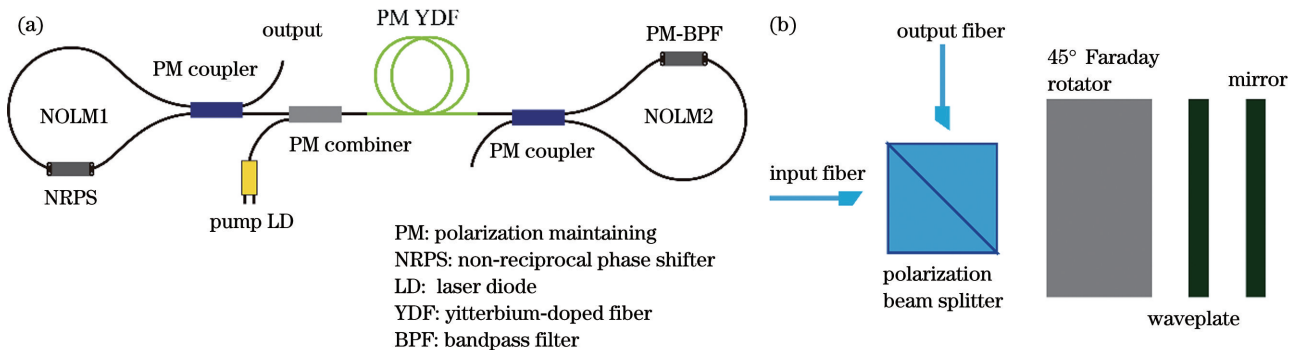


图 1 激光器结构示意图。(a) 全保偏哑铃形锁模光纤激光器;(b) NRPS

Fig. 1 Schematic of laser structure. (a) Dumbbell-shaped all-polarization-maintaining mode-locked fiber laser; (b) NRPS

当泵浦功率较低时,激光器运行在连续波状态下;泵浦功率升高到 $2.1\ \text{W}$,激光器进入锁模状态;降到 $1.8\ \text{W}$,激光器失锁。图 2 展示了泵浦功率为 $1.8\ \text{W}$ 时输出脉冲的时域、频域状态,此时激光器输出脉冲宽度最窄。图 2(a) 所示为输出激光脉冲的光谱,其中心波长为 $1064\ \text{nm}$, $3\ \text{dB}$ 带宽为 $1.3\ \text{nm}$,光谱形状呈三角形;图 2(b) 所示为输出脉冲的单脉冲波形,使用 $45\ \text{GHz}$ 带宽的 InGaAs 探测器采集并使用 $60\ \text{GHz}$ 带宽的采样示波器测量,示波器的触发信号由 $1.5\ \text{GHz}$ 探测器提供。可以看出,脉冲形状为边沿陡峭的近似平顶矩形,脉冲宽度为 $156\ \text{ps}$ 。图 2(c) 和插图所示分别为 $9\ \text{MHz}$ 和 $0.8\ \text{GHz}$ 扫描范围下的脉冲射频谱,其输出脉冲射频谱信噪比高达 $57\ \text{dB}$,说明脉冲序列幅值具有很高的稳定性。图 2(d) 所示为 $1.5\ \text{GHz}$ 实时示波器测量的脉冲序列波形,其锁模脉冲为单脉冲,脉冲周期为 $123\ \text{ns}$,对应的重复频率为 $8.1\ \text{MHz}$,与激光上述相符合,可以判断此时激光器运行在耗散孤子共

器等效腔长基本匹配。根据 $106\ \text{mW}$ 的平均功率和 $8.1\ \text{MHz}$ 的重复频率,可以计算得到此时的脉冲能量为 $13\ \text{nJ}$,峰值功率为 $84\ \text{W}$ 。

继续增大泵浦功率,输出脉冲的脉冲宽度和脉冲能量随之线性增加,同时脉冲峰值功率和重复频率基本保持不变。图 3(a) 所示为泵浦功率从 $2.7\ \text{W}$ 增大到最高值 $22.7\ \text{W}$ 时激光器输出脉冲波形的变化情况,其中 5 条曲线对应的输出脉冲宽度分别为 $1.0, 2.0, 4.0, 6.0, 8.1\ \text{ns}$ 。图 3(b) 所示为激光器输出平均功率、脉冲宽度和峰值功率随泵浦功率的变化曲线。可以看出,当泵浦功率从 $1.8\ \text{W}$ 增加到 $22.7\ \text{W}$ 时,输出脉冲宽度从 $156\ \text{ps}$ 线性增加到 $8.1\ \text{ns}$,激光器输出平均功率从 $106\ \text{mW}$ 线性增加到 $5.5\ \text{W}$,相应的脉冲能量从 $13\ \text{nJ}$ 线性增加到 $0.68\ \mu\text{J}$ 。其平顶矩形脉冲的波形、脉冲宽度和能量随泵浦功率升高而线性增大、不发生脉冲分裂的特性与 Chang 等^[1]对耗散孤子共振锁模的特征描述锁模状态下。

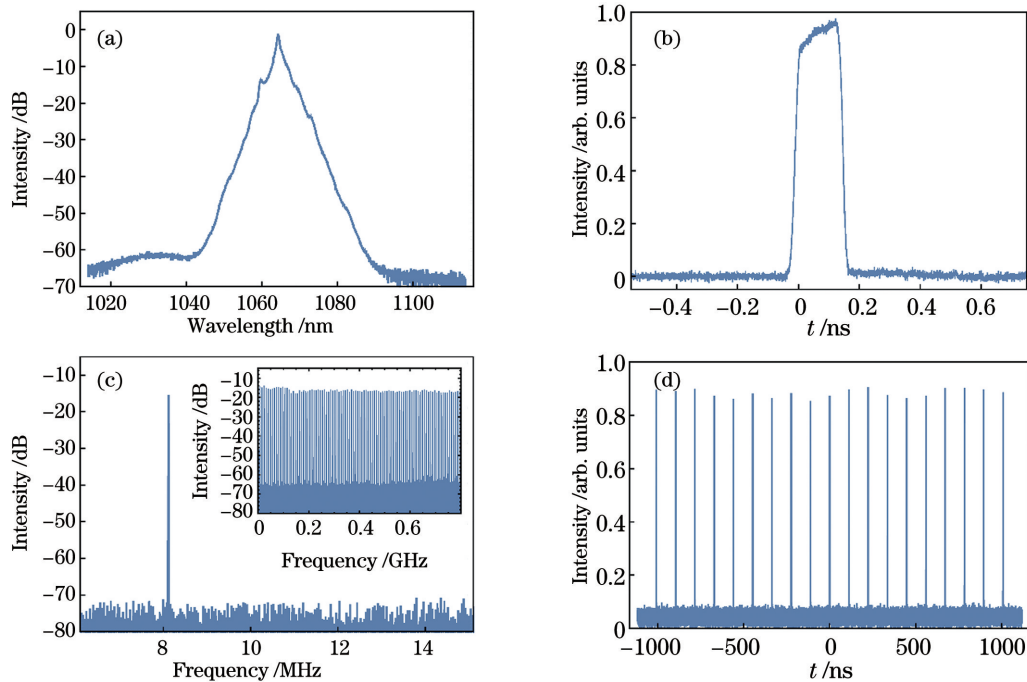


图 2 泵浦功率为 1.8 W 时激光器的输出特性。(a) 光谱; (b) 单脉冲波形; (c) 9 MHz 和 0.8 GHz (插图) 范围内的射频谱; (d) 脉冲序列波形

Fig. 2 Output characteristics of the laser under the pump power of 1.8 W. (a) Optical spectrum; (b) single pulse waveform; (c) radio frequency spectra in the span of 9 MHz and 0.8 GHz (inset); (d) pulse train waveform

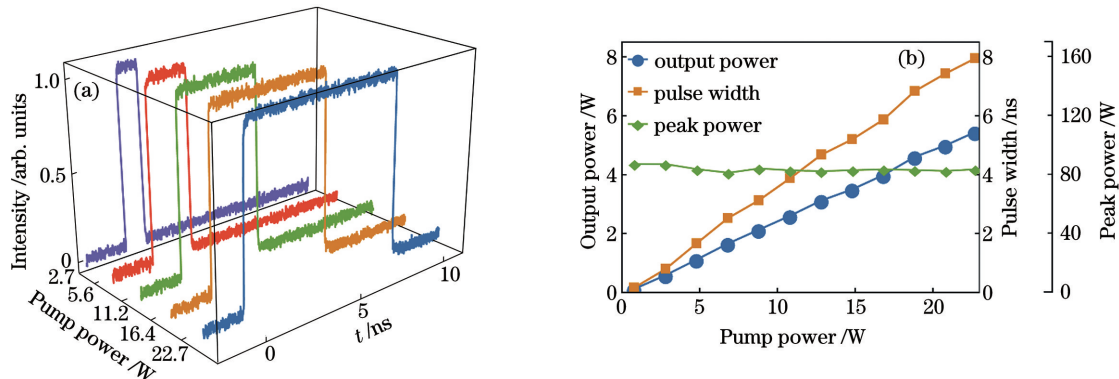


图 3 脉冲波形、平均功率、脉冲宽度和峰值功率随泵浦功率的变化情况。(a) 输出脉冲波形的变化; (b) 平均功率、脉冲宽度和峰值功率的变化曲线

Fig. 3 Variations of the pulse waveforms, average power, pulse width, and peak power with pump power. (a) Variations of output pulse waveforms; (b) variation curves of the output average power, pulse width, and peak power

实验中任意摆放关键器件或对连接光纤进行重新排布和抖动,都不会对激光器输出状态产生明显影响。通过妥善处理关键节点的散热,最高输出功率下激光器关键器件和光纤温度都能稳定在 $60\text{ }^{\circ}\text{C}$ 以下,无需额外的主动制冷装置。50 次以上的开关实验中锁模正常启动成功率达到 100%。相比于此前公开报道的全光纤掺镱锁模谐振腔的最高输出功率,所设计激光器在平均功率上实现了超过 1 倍的提升^[2-3],脉冲能量也有明显提升,而且得益于优化的全保偏哑铃形结构,激光器实现了免调试运行并

表现出良好的稳定性、抗干扰能力和自启动性能。下一步工作的重点是通过优化结构来产生高功率、大能量的超快脉冲。

参 考 文 献

- [1] Chang W, Ankiewicz A, Soto-Crespo J M, et al. Dissipative soliton resonances [J]. *Physical Review A*, 2008, 78(2): 023830.
- [2] Huang Y Z, Luo Z Q, Xiong F F, et al. Direct generation of 2 W average-power and 232 ns picosecond pulses from an ultra-simple Yb-doped

- double-clad fiber laser[J]. *Optics Letters*, 2015, 40 (6): 1097-1100.
- [3] Guo Y Y, Xu Y, Zhang J J, et al. High-power dissipative soliton resonance fiber laser with compact linear-cavity configuration[J]. *Optik*, 2019, 181: 13-17.
- [4] Szczepanek J, Kardaś T M, Michalska M, et al. Simple all-PM-fiber laser mode-locked with a nonlinear loop mirror[J]. *Optics Letters*, 2015, 40 (15): 3500-3503.
- [5] Jiang T X, Cui Y F, Lu P, et al. All PM fiber laser mode locked with a compact phase biased amplifier loop mirror[J]. *IEEE Photonics Technology Letters*, 2016, 28(16): 1786-1789.
- [6] Zhou J Q, Pan W W, Zhang L, et al. Research advances in mode-locked fiber lasers based on nonlinear loop mirror[J]. *Chinese Journal of Lasers*, 2019, 46(5): 0508013.
周佳琦, 潘伟巍, 张磊, 等. 非线性环路反射镜锁模光纤激光器的研究进展[J]. *中国激光*, 2019, 46 (5): 0508013.
- [7] Krzempek K, Tomaszewska D, Abramski K M. Dissipative soliton resonance mode-locked all-polarization-maintaining double clad Er : Yb fiber laser[J]. *Optics Express*, 2017, 25 (21): 24853-24860.
- [8] Chen H, Chen S P, Jiang Z F, et al. 0.4 μJ , 7 kW ultrabroadband noise-like pulse direct generation from an all-fiber dumbbell-shaped laser [J]. *Optics Letters*, 2015, 40(23): 5490-5493.
- [9] Chen H, Chen S P, Jiang Z F, et al. 80 nJ ultrafast dissipative soliton generation in dumbbell-shaped mode-locked fiber laser[J]. *Optics Letters*, 2016, 41 (18): 4210-4213.
- [10] Cai J H, Chen S P, Hou J. Square pulses from an all-polarization-maintained dumbbell-shaped fiber laser [C] // 2017 16th International Conference on Optical Communications and Networks (ICOON), August 7-10, 2017, Jiaying, China. New York: IEEE Press, 2017: 1-3.

High-Power All-Polarization-Maintaining Large-Mode-Area Dumbbell-Shaped, Ytterbium-Doped Mode-Locked Fiber Laser

Chen He^{1*}, Zhou Feng¹, Lei Chengmin¹, Cai Junhao², Chen Shengping²

¹93236 Troops of Chinese People's Liberation Army, Beijing 100085, China;

²College of Advanced Interdisciplinary Studies, National University of Defense Technology, Changsha, Hunan 410073, China

Abstract

Objective Passively mode-locked fiber lasers have been widely studied because of their simple structure, low cost, and high reliability. All-fiber passively mode-locked fiber lasers have outstanding advantages in terms of stability, reliability, and packaging technology because of the absence of spatial optical components. Their output pulse energy and average power are generally low because of fiber nonlinearity and poor power tolerance ability of fiber devices. To improve their pulse energy and average power while ensuring strong anti-interference stability, we developed an all-fiber all-polarization-maintaining dumbbell-shaped, ytterbium (Yb)-doped mode-locked fiber laser based on the nonlinear optical loop mirror (NOLM) dumbbell-shaped structure. By introducing all-polarization-maintaining large-mode-area fiber, high-power fiber components, and optimized cavity, we realized an average power of 5.5 W and pulse energy of 0.68 μJ in rectangular dissipative soliton resonance mode-locking.

Methods Figure 1(a) shows the laser structure, comprising an amplifier and two equivalent cavity mirrors composed of NOLMs. The NOLM1 on the left has a coupling ratio of 10:90, and a nonreciprocal phase shifter (NRPS) with a phase shift of $3\pi/4$ is inserted into the ring. The NOLM2 on the right has a coupling ratio of 50:50, and a bandpass filter with a center wavelength of 1064 nm and a 3-dB bandwidth of 13 nm is connected to the ring. All the fibers in the cavity are single-mode, polarization-maintaining large-mode-area double-clad fibers with a core diameter and a numerical aperture of 10 μm and 0.08, respectively, which can reduce the nonlinear effects in the cavity. NOLM1 acts as an equivalent output cavity mirror and an equivalent saturable absorber, whereas the bandpass filter added in the NOLM2 stabilizes the laser center wavelength and dissipates soliton resonance. The insertion of NRPS can change the reflective NOLM's power-dependent reflectivity curve to achieve saturated absorption characteristics. A reasonable selection of NRPS phase shifts can also change the self-starting performance

of NOLM-based mode-locked lasers.

Results and Discussions When the pump power of the laser is low, it runs in continuous wave state. When the pump power increases to 2.1 W, the laser turns to a mode-locked state, and when it drops to 1.8 W, it goes to a continuous wave state. Figure 2 shows the output pulse's characteristics at 1.8-W pump power. Moreover, the pulse shape is approximately a flat-topped rectangle with steep edges, with pulse width of 156 ps, repetition frequency of 8.1 MHz, pulse energy of 13 nJ, and peak power of 84 W. When the pump power is increased, the pulse width and the output pulse energy increase linearly, and the pulse peak power and repetition frequency remain unchanged. Figure 3 shows the variations of the pulse waveforms, average power, pulse width, and peak power at different pump powers. When the pump power is increased from 1.8 to 22.7 W, the output pulse width linearly increases from 156 ps to 8.1 ns, the average laser output power from 106 mW to 5.5 W, and the corresponding pulse energy from 13 nJ to 0.68 μ J. Hence, it can be concluded that the laser is operating in the dissipative soliton resonance mode-locked state.

Conclusions On the basis of an all-fiber, all-polarization-maintaining dumbbell-shaped, Yb-doped mode-locked fiber laser, we realized a high-power large-energy rectangular dissipative soliton resonance mode-locking. The pulse width can be adjusted from 156 ps to 8.1 ns. When the pump power reached 22.7 W, the average output power, pulse energy, and peak power increased to 5.5 W, 0.68 μ J, and 84 W, respectively. Benefiting from the all-polarization maintaining structure, we found that the laser exhibited excellent anti-interference stability. Compared with the previously reported maximum output power of all-fiber, Yb-doped mode-locked resonators, we achieved an increase of more than 100% in the average power and a significantly improved pulse energy.

Key words lasers; fiber lasers; mode-locked lasers; dissipative soliton resonance; nonlinear optical loop mirror; dumbbell-shaped lasers

OCIS codes 140.3510; 140.4050; 140.3615; 320.7090